

Fusion cross section of light ions at sub-Coulomb energies

J.-L. Dethier

Institut de Physique, Sart Tilman, B-4000 Liège 1, Belgium

Fl. Stancu

*Institut de Physique, Sart Tilman, B-4000 Liège 1, Belgium
and Nuclear Physics Laboratory, Keble Road, Oxford OX1 3RH, United Kingdom*

(Received 9 July 1980)

We investigate a barrier penetration model for the sub-Coulomb fusion of light ion systems and derive an analytic formula for the cross section. The validity of the model is checked against results based on a modified proximity potential which reproduces the fusion cross section at energies above the Coulomb barrier. The meaning of the parameters defining the model as well as the extrapolation of the formula at very low energies are discussed.

[NUCLEAR REACTIONS Analytic expression of fusion cross section in a barrier penetration model.]

I. INTRODUCTION

At low energies it is assumed that the fusion cross section is identical to the reaction cross section, and that the calculations can be reduced to a barrier penetrability problem. The shape of the barrier depends on the choice of the nuclear and Coulomb potentials. An example is shown in Fig. 1 for the system $^{16}\text{O} + ^{16}\text{O}$. The potential V_l is defined in Sec. III A. One can see that for partial waves $l < 22$ the potential has a pocket, i.e., a minimum, followed by a barrier situated around the maximum of V_l . For $l \geq 22$, where the pocket has disappeared, the formalism presented below is no more valid. Several choices have been considered for the nuclear and Coulomb potentials [cf. Refs. 1-4]. Among these choices, it turns out that at energies above the Coulomb barrier ($l=0$) the proximity potential,⁵ with a small adjustment¹ of one parameter, can well account for the fusion cross section up to bombarding energies corresponding to partial wave barriers where the potential still has a pocket. Other adjustments^{2,4} are consistent with,¹ and almost always imply, an increase in the attraction of the original proximity potential. Instead of directly working with a chosen barrier, as in Fig. 1, a common and convenient procedure is to approximate the potential in the barrier region with a parabola which gives an analytic form of the transmission coefficient.⁶ The parabola is fitted to reproduce the position, height, and curvature of the real barrier, and in Refs. 1 and 2 the importance of fitting a parabola for each partial wave was shown.

The parabolic barrier is a good approximation for energies near and above the top of the Coulomb barrier. For energies well below the Coulomb

barrier, the much slower decrease of the Coulomb tail with respect to a parabola fitted at the top of the barrier [see Figs. 2(a) and 2(b)] suggests that the parabolic barrier approximation is inadequate. Recently Avishai⁷ proposed a

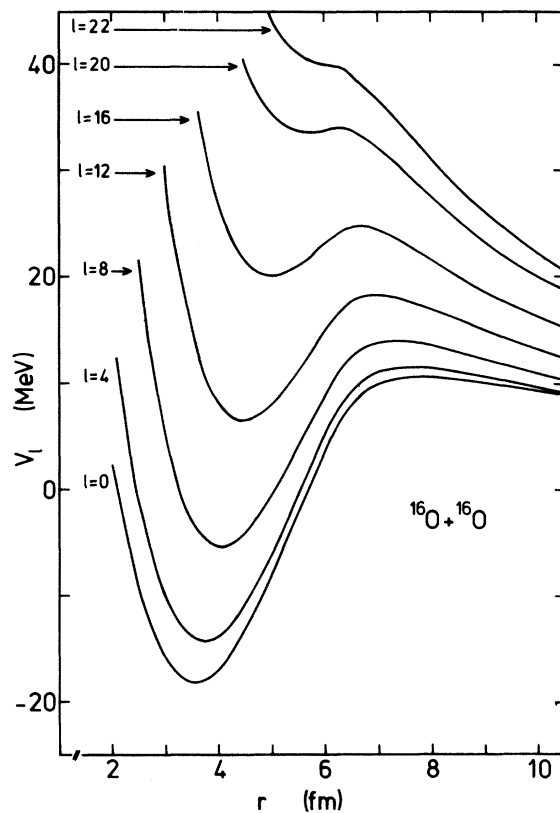


FIG. 1. Effective potential V_l for $^{16}\text{O} + ^{16}\text{O}$ as a function of the relative distance r between nuclear centers. V_l is the sum of a modified proximity potential (see text), a Coulomb term, and a centrifugal term.

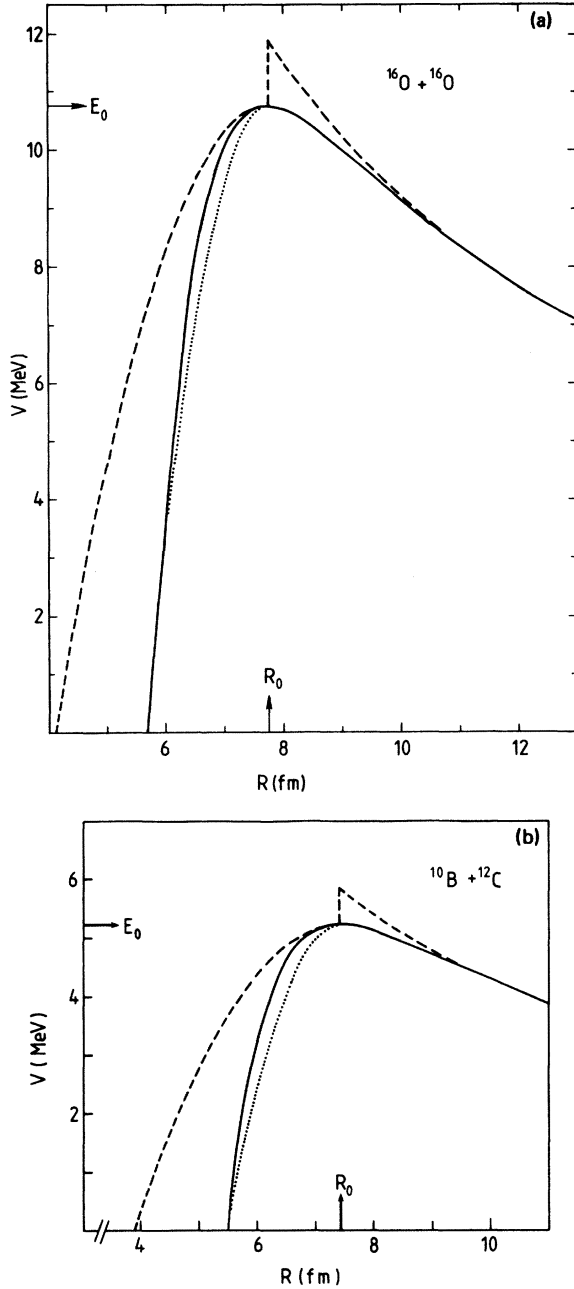


FIG. 2. (a) Potential barrier $V = V_N + V_C$ for $^{16}\text{O} + ^{16}\text{O}$. Full line is with the modified proximity potential V_N as in Ref. 1 and Coulomb potential V_C as in Ref. 8. The dashed line is the model of Eq. (4) with parameters given in columns 2–4 of Table I and the dotted parabola has $\hbar\omega_0$ from column 5 of Table I instead of column 4. (b) Same as (a) but for $^{12}\text{C} + ^{10}\text{B}$.

model which takes into account the Coulomb tail and still gives an analytic form of the transmission coefficient. For $l=0$ it consists of replacing the half of the parabola to the right side of the barrier top by a Coulomb potential between two

point charges. In the present paper we analyze the applicability of the model proposed by Avishai. We compare its results with those obtained from a realistic barrier formed from the Coulomb potential of Ref. 8 and the nuclear proximity potential adjusted as in Ref. 1. We propose a modification of Avishai's model to take into account the centrifugal term on both sides of the barrier and study an approximation which leads to analytic expressions for the transmission coefficient and the cross section.

In the next section we present the model. By introducing some approximations we derive an expression for the fusion cross section. In Sec. III we show by numerical examples the validity of various approximations involved and discuss the choice of the parameters defining the model. In Sec. IV we analyze the fit to experimental sub-Coulomb fusion data, and in Sec. V we conclude the paper.

II. THE MODEL

At low energies the gross structure of the fusion cross section is well accounted for by the formula

$$\sigma_F = \pi \lambda^2 \sum_{l=0}^{\infty} (2l+1) T_l, \quad (1)$$

where λ is the reduced wavelength of the relative motion and T_l the transmission coefficient for the partial wave l . We calculate T_l from the expression⁹

$$T_l = \frac{1}{1 + \exp(2K_l)}, \quad (2)$$

where K_l is the penetrability integral through the barrier $V_l(r)$,

$$K_l = \int_{r_1}^{r_2} \left(\frac{2\mu}{\hbar^2} [V_l(r) - E] \right)^{1/2} dr, \quad (3)$$

r_1 and r_2 being the turning points at the bombarding energy E in the center of mass system, and μ is the reduced mass. The form (2) of T_l results from a semi-classical approximation. In the limit of large K_l it turns into the more familiar WKB expression.

Consider a potential $V_l = V_0 + \hbar^2(l + \frac{1}{2})^2 / 2\mu r^2$. If the maximum of V_0 is positioned at R_0 , we assume that in the barrier region the shape of V_l can be approximated by

$$V_l \approx E_0 - \mu \omega_0^2 \frac{(r - R_0)^2}{2} + \frac{\hbar^2(l + \frac{1}{2})^2}{2\mu r^2}, \quad r < R_0 \quad (4)$$

$$\approx \frac{Z_1 Z_2 e^2}{r} + \frac{\hbar^2(l + \frac{1}{2})^2}{2\mu r^2}, \quad r > R_0,$$

i.e., the inner side ($r < R_0$) of the Coulomb barrier ($l=0$) is a half-parabola of height E_0 and curvature

$\hbar\omega_0$, and the outer side ($r > R_0$) is a pure Coulomb repulsion between two point charges. The difference with respect to Avishai's model⁷ is that a centrifugal term is added for $r > R_0$ and the same term is considered a function of r for $r < R_0$, instead of a constant. If E_0 and R_0 are taken from systematics of fusion cross section (see, e.g., Ref. 1), then the function (4) has a discontinuity at R_0 which increases with $Z_1 Z_2$ and makes the model less adequate for larger nuclei. For light heavy ions at bombarding energies well below the barrier top, the effect of this discontinuity is negligible, as we shall see below.

The integral K_1 can be evaluated exactly for $R_0 < r < r_2$, but it would be advantageous to have an analytic expression for the whole integration interval. This can be obtained approximately by making a series expansion of the integrand in terms of the centrifugal term. Keeping the first term in the expansion, we obtain

$$K_1 \simeq K_0(E) + (l + \frac{1}{2})^2 [D_p(E) + D_c(E)], \quad (5)$$

where

$$K_0 = \frac{\pi(E_0 - E)}{2\hbar\omega_0} + \pi\eta - 2\eta \arcsin\left(\frac{kR_0}{2\eta}\right)^{1/2} - [kR_0(2\eta - kR_0)]^{1/2}, \quad (6)$$

$$D_p = \frac{\hbar}{2\mu\omega_0 R_0^2} \left(\frac{x}{1-x^2} + \frac{\pi/2 + \arcsin x}{(1-x^2)^{3/2}} \right), \quad (7)$$

and

$$D_c = \frac{1}{2\eta} \left(\frac{2\eta}{kR_0} - 1 \right)^{1/2}. \quad (8)$$

In the expressions above η is the Sommerfeld parameter $\eta = \mu Z_1 Z_2 e^2 / \hbar^2 k$, k is the wave number, and

$$x^2 = \frac{2(E_0 - E)}{\mu\omega_0^2 R_0^2}. \quad (9)$$

In K_0 the first term represents the integration over the half-parabola and the other terms result from the integration over the Coulomb tail. This is the $l=0$ contribution. The $l \neq 0$ partial waves give an additional term in (5), where D_p and D_c come from the first derivative of K_1 with respect to $(l + \frac{1}{2})^2$ integrated from r_1 to R_0 and R_0 to r_2 , respectively. Avishai's result can be considered as a particular case of Eqs. (5)-(8) and is obtained by setting $D_c = 0$ and $x = 0$. The approximation $x \simeq 0$ is good for a narrow parabola (large $\hbar\omega_0$) having a height $E_0 \ll \mu\omega_0^2 R_0^2 / 2$. Such examples are the parabolas with parameters taken from columns 2, 3, and 5 of Table I, which give $x \leq 0.07$. Setting $x \simeq 0$ the quantity D_p becomes

$$D_p = \frac{\hbar^2}{4\mu R_0^2 \hbar\omega_0} \pi. \quad (7')$$

TABLE I. Parameters of the model of Eqs. (4).

Pair	E_0 (MeV)	R_0 (fm)	$\hbar\omega_0^a$ (MeV)	$\hbar\omega_0^b$ (MeV)	$\hbar\omega_0^c$ (MeV)
$^{16}\text{O} + ^{16}\text{O}$	10.75	7.74	2.92	5.08	3.54
$^{16}\text{O} + ^{14}\text{N}$	9.05	8.08	2.72	4.95	3.23
$^{16}\text{O} + ^{12}\text{C}$	7.94	7.88	2.69	4.90	3.26
$^{14}\text{N} + ^{12}\text{C}$	6.99	7.83	2.61	4.77	3.19
$^{12}\text{C} + ^{12}\text{C}$	6.36	7.31	2.66	4.81	3.44
$^{11}\text{B} + ^{12}\text{C}$	5.21	7.46	2.46	4.44	3.14
$^{10}\text{B} + ^{12}\text{C}$	5.23	7.43	2.51	4.57	3.24

^aFrom Ref. 1.

^bFrom fitting the inner part of the barrier at one point (see text).

^cFrom Eq. (18).

This is Avishai's expression for D_p , convenient for narrow parabolas. But there are no arguments to neglect D_c , which is of the same order of magnitude and usually greater than D_p .

One would expect the approximation (5) to be valid whenever the increase in the area under the barrier due to the centrifugal term is small compared to the $l=0$ barrier. This happens for low partial waves and at energies well below the top of the Coulomb barrier. A detailed numerical analysis is given in the next section.

Finally, using the approximation (5) for K_1 , one can write a closed formula for the fusion cross section (1) by replacing the sum with an integral over l . This gives the expression

$$\sigma_F = \frac{\pi\kappa^2}{2(D_p + D_c)} \ln[1 + \exp(-2K_0)], \quad (10)$$

which is an analog of Wong's formula¹⁰ (see the Appendix) valid at energies around and above the Coulomb barrier. Wong assumed parabolic shapes for all barriers with the same parameters R_0 , $\hbar\omega_0$ in all partial waves. Recent studies^{1,2} have shown that the dependence on l of the parameters defining the parabola is important at energies above the Coulomb barrier. For the model studied in the present paper one has to define the parabola parameters for $l=0$ only. The approximations which lead to formula (10) are studied numerically in the next section.

III. DISCUSSION

Presently we discuss the validity of the model described in the previous section by performing a numerical analysis of the approximations used in deriving the expression (10) for the fusion cross section.

First we have to choose a realistic barrier whose shape will be approximated by the Eqs. (4). This is done in Sec. III A. Second we have

to find values of the parameters R_0 , E_0 , and $\hbar\omega_0$ which fit the realistic barrier. This is discussed in the Sec. III B. Lastly the validity of the approximations used to derive the cross section formula is analyzed in Sec. III C.

The intention of the present work is to understand the model (4) rather than experimental data. However, a comparison with the measured cross sections will be given in Sec. IV.

A. The "exact" barrier

We consider the potential

$$V_i(r) = V_N(r) + V_C(r) + \frac{\hbar^2(l + \frac{1}{2})^2}{2\mu r^2}, \quad (11)$$

where V_N is the nuclear part and V_C the Coulomb part. For V_N we choose the modified version of the proximity potential⁵ as proposed by Vaz and Alexander¹

$$V_N(\xi) = 4\pi\gamma b C_1 C_2 / (C_1 + C_2) \phi(\xi), \quad (12)$$

$$\xi = (r - C_1 - C_2)/b,$$

where ξ is the dimensionless separation distance between nuclear surfaces, $b = 1$ fm a parameter related to the surface thickness, and $\phi(\xi)$ a universal function expressed analytically as

$$\begin{aligned} \phi(\xi) &= -0.5(\xi - 2.54)^2 - 0.0852(\xi - 2.54)^3, \quad \xi \leq 1.2511 \\ &= -3.437 \exp(-\xi/0.75), \quad \xi \geq 1.2511. \end{aligned} \quad (12')$$

The parameters C_i are the central radii related to the effective sharp radii R_i by

$$C_i = R_i - b^2/R_i, \quad (12'')$$

$$R_i = 1.28A_i^{1/3} - 0.76 + 0.8A_i^{-1/3} + \Delta R \quad (i=1, 2),$$

where ΔR is explained below. The quantity γ is the surface energy coefficient given by

$$\gamma = 0.9517 \left[1 - 1.7826 \left(\frac{N-Z}{A} \right)^2 \right].$$

The Coulomb potential V_C is taken as in Ref. 8.

$$\begin{aligned} V_C &= V_0 - kr^n \text{ for } r \leq R_1 + R_2, \\ V_0 &= \frac{3e^2}{5} \left(\frac{(Z_1 + Z_2)^2}{(R_1^3 + R_2^3)^{1/3}} - \frac{Z_1^2}{R_1} - \frac{Z_2^2}{R_2} \right), \\ n &= \left(\frac{V_0(R_1 + R_2)}{Z_1 Z_2 e^2} - 1 \right)^{-1}, \\ k &= \left(V_0 - \frac{Z_1 Z_2 e^2}{R_1 + R_2} \right) (R_1 + R_2)^{-n}, \end{aligned} \quad (13)$$

and

$$V_C = \frac{Z_1 Z_2 e^2}{r} \text{ for } r \geq R_1 + R_2. \quad (13')$$

This Coulomb potential is more adequate for heavy ion collisions than that used in Ref. 1, but this choice does not alter the results obtained there because in the energy range considered, the fusion cross section is insensitive to the inner part of the barrier.

Vaz and Alexander¹ indicated that small changes in the values of the parameters R_i , γ , or b as proposed by Błocki *et al.*⁵ were necessary in order to obtain a good fit of the fusion cross section at energies above the Coulomb barrier. From a detailed numerical study they found that a change in all three parameters is practically equivalent to a change in one parameter only. They found it convenient to adjust the radii R_i as defined in Ref. 5 by a quantity ΔR . In formula (12') we use for ΔR values taken from Table II of Ref. 1.

In Ref. 1 each V_i was approximated by a parabola with l dependent parameters E_i , R_i , and $\hbar\omega_i$, and the transmission coefficient T_i was calculated according to the Hill-Wheeler formula,⁶

$$T_i(E) = \left(1 + \exp \frac{2\pi(E_i - E)}{\hbar\omega_i} \right)^{-1}. \quad (2')$$

This is a very good approximation for energies around and above the Coulomb barrier as long as V_i has a pocket and the values of E_i , R_i , and $\hbar\omega_i$ were determined once the parameters ΔR were adjusted. The model studied in this paper needs parameters for $l=0$ only, and it would be interesting to see if the values found by Vaz and Alexander retain a meaning at energies well below the barrier.

B. Parameters of the model

We apply the model to a series of pairs of light ions which are of particular interest in astrophysics and for which there are extensive measurements of the fusion cross section at sub-Coulomb energies.¹¹

The pairs of nuclei under discussion are given in Table I together with the parameters E_0 , R_0 , and $\hbar\omega_0$ used in the calculations. The values of E_0 and R_0 are the same as in Ref. 1. For $\hbar\omega_0$ we leave some freedom. One choice is to take it as in Ref. 1. Such values are reproduced in column 4 of Table I. By definition they give half-parabolas with the same curvature at R_0 as that of the exact potential defined in Sec. III A. But, as one can see from Figs. 2(a) and 2(b), there is a large difference between the half-parabola (dashed line) and the exact potential (full line) at $r < R_0$. At bombarding energies well below the barrier this difference affects considerably the penetrability integral (3). Two typical cases are

shown in Tables II and III for $^{16}\text{O}+^{16}\text{O}$ at $E_{\text{c.m.}} = 7.76$ MeV and $^{10}\text{B}+^{12}\text{C}$ at $E_{\text{c.m.}} = 1.22$ MeV, respectively. One should compare columns 2 and 5 which give the double of the penetrability integral calculated with the dashed half-parabola and the exact barrier, respectively. For the partial waves indicated in the tables one can see that with increasing l the model overestimates the penetrability integral from 15% to ~30% for $^{16}\text{O}+^{16}\text{O}$ and from 7% to 9% for $^{12}\text{C}+^{10}\text{B}$. It seems therefore necessary to look for an $\hbar\omega_0$ which would better reproduce the area of the exact potential, and hence give more satisfactory values for K_l . An appropriate way is to make the parabola intersect the r axis at the same place as the exact potential does. This recipe gives the values of $\hbar\omega_0$ indicated in column 5 of Table I. In Tables II and III, column 3, one can find the corresponding penetration integrals. As before, the partial waves considered give the major contribution to the fusion cross section of $^{16}\text{O}+^{16}\text{O}$ and $^{12}\text{C}+^{10}\text{B}$ at the indicated energies. Compared to column 2 the values of column 3 deviate much less from the exact values K_l^E , i.e., by 1% to 1.5%. An important result to be noticed is that the penetrability integrals K_l^A evaluated with the approximation (5) and given in column 4 are very close to the values of K_l in column 3, i.e., those obtained without making any series expansion. Some small deviations appear for large values of l but the contribution of these partial waves to the total cross section is very small. Therefore it seems perfectly justified to use the approximation (5) for K_l . We recall that the formula (10) for the total cross section is based on this approximation and on the transformation of the sum over l into an integral. The effect of both these approximations on the cross section will be discussed in the next paragraph.

In Tables II and III we also give results for

partial cross section

$$\sigma_l = \pi\lambda^2(2l+1)T_l.$$

In columns 6 and 7, σ_l comes from a T_l calculated with K_l^A and K_l^E , respectively. It turns out that differences of 2-3% between K_l^A and K_l^E change the partial cross section for the largest partial waves by 50%. But, as it is shown in the last column, these partial waves give a very small contribution to the total cross section.

C. Cross section

Results for the total cross section are given in Tables IV-VI for $^{16}\text{O}+^{16}\text{O}$, $^{14}\text{N}+^{12}\text{C}$, and $^{10}\text{B}+^{12}\text{C}$ at several values of the energy below the Coulomb barrier. Columns 2-4 represent the sequence of approximations used to derive the analytic formula (10) for σ_F . It is meaningful to compare each of these columns with column 5, which gives the fusion cross section σ_F^{prox} obtained from the potential of Sec. III A by making a summation over all contributing partial waves. As was expected, the model (4) cannot be applied just below E_0 because of the artificial kink in the barrier see Figs. 2(a) and 2(b). Indeed, in the case of $^{16}\text{O}+^{16}\text{O}$, one can see that at $E_{\text{c.m.}} = 9.76$ MeV, i.e., at ~1 MeV below the barrier top, the fusion cross section in columns 2-4 is smaller by ~12% than the exact cross section σ_F^{prox} . Just below the Coulomb barrier the parabolic approximation of Eq. (2') would be more adequate. Column 2 gives the cross section for the barrier (4) with parameters from columns 2, 3, and 5 of Table I. The penetrability integral is calculated exactly for each partial wave and the cross section is calculated from Eqs. (1)-(3). At energies of a few MeV below the Coulomb barrier the model gives larger cross sections

TABLE II. Results for the penetrability integral K_l and partial fusion cross section σ_l of $^{16}\text{O}+^{16}\text{O}$ at $E_{\text{c.m.}} = 7.76$ MeV. Column 2—with parameters from Ref. 1; column 3—with a semiparabola which fits well the inner side of the exact barrier; column 4—as in column 3 but with the approximation (5); column 5—with the exact barrier of Ref. 1; column 6—the partial fusion cross section with approximation (5); column 7—the partial fusion cross section for the exact potential; column 8—ratio of the partial to total fusion cross section for the exact barrier Ref. 1.

l	$2K_l$ ($\hbar\omega_0 = 2.92$)	$2K_l$ ($\hbar\omega_0 = 5.08$)	$2K_l^A$ ($\hbar\omega_0 = 5.08$)	$2K_l^E$	σ_l^A (mb)	σ_l^E (mb)	σ_l^E/σ^E
0	9.563	8.202	8.202	8.336	2.88×10^{-3}	2.52×10^{-3}	0.11
2	10.403	8.825	8.824	8.994	7.73×10^{-3}	6.52×10^{-3}	0.27
4	12.465	10.295	10.275	10.520	3.26×10^{-3}	2.55×10^{-3}	0.11
6	16.155	12.643	12.556	12.897	4.81×10^{-4}	3.42×10^{-4}	0.01
8	∞	15.928	15.666	16.138	2.80×10^{-5}	1.75×10^{-5}	0.0007

TABLE III. Same as Table II but for $^{12}\text{C} + ^{10}\text{B}$ at $E_{c.m.} = 1.22$ MeV.

l	$2K_l$ ($\hbar\omega_0 = 2.51$)	$2K_l$ ($\hbar\omega_0 = 4.57$)	$2K_l^A$ ($\hbar\omega_0 = 4.57$)	$2K_l^E$	σ_l^A (mb)	σ_l^E (mb)	σ_l^E/σ^E
0	32.598	30.339	30.339	30.578	6.529×10^{-12}	5.142×10^{-12}	0.23
1	33.348	30.859	30.859	31.090	1.165×10^{-11}	0.924×10^{-11}	0.42
2	34.967	31.898	31.898	32.106	6.869×10^{-12}	5.580×10^{-12}	0.25
3	∞	33.460	33.457	33.611	2.024×10^{-12}	1.734×10^{-12}	0.08
4	∞	35.557	35.535	35.588	3.256×10^{-13}	3.086×10^{-13}	0.01
5	∞	38.227	38.133	38.037	2.962×10^{-14}	3.258×10^{-14}	0.001
6	∞	41.575	41.250	40.979	1.550×10^{-15}	2.032×10^{-15}	0.0001

than the exact barrier, because at these energies the area under the penetrability integral is smaller for the model than for the exact barrier. For even lower energies the difference in the area becomes less important with respect to the total area and the results of the model become closer to those of the exact barrier. Column 3 shows the effect of the approximation (5) in the penetrability integral. One can see that this approximation is very good except for energies of 1 MeV or less below the Coulomb barrier, where the model is not reliable. Column 4 is the result of Eq. (10). The transformation of the sum into an integral for obtaining Eq. (10) brings an artificial contribution of a continuously varying l and slightly reduces the total cross section. This decrease somewhat compensates for the increase produced by the model itself. Then formula (10) brings a maximum error of $\sim 20\%$ for $^{16}\text{O} + ^{16}\text{O}$ or $^{10}\text{B} + ^{12}\text{C}$ in the energy range of 3–4 MeV below the Coulomb barrier. In other cases, e.g., $^{12}\text{C} + ^{16}\text{O}$ or $^{14}\text{N} + ^{12}\text{C}$, this figure rises up to $\sim 30\%$ and gives an average maximum error (overestimate) of $\sim 25\%$. After reaching a maximum this error decreases for lower values of E .

IV. COMPARISON WITH THE EXPERIMENT

The relation between the exact barrier and its approximation by the present model being established, we can now discuss the comparison with the experiment. We consider the data of Ref. 11,

which refer to the S factor related to the fusion cross section by

$$S = \sigma_F E e^{2\pi\eta} \quad (14)$$

Figure 3 shows these data together with results obtained by calculating σ_F with formula (10) and parameters from columns 2, 3, and 5 of Table I. The last column of Tables IV–VI indicates the S factor obtained for $^{16}\text{O} + ^{16}\text{O}$, $^{14}\text{N} + ^{12}\text{C}$, and $^{10}\text{B} + ^{12}\text{C}$, respectively. We notice that the proximity potential gives smaller values for S than its approximation by the model (4), the ratio between the S factors being the same as the ratio between the associated cross sections. For all pairs except $^{16}\text{O} + ^{16}\text{O}$ one obtains the correct order of magnitude for S . The agreement between the calculations and the experiment can be improved by increasing the value of $\hbar\omega_0$, for example up to ~ 7 MeV for $^{14}\text{N} + ^{12}\text{C}$, and ~ 6.5 MeV for $^{10}\text{B} + ^{12}\text{C}$. This suggests that a potential with a steeper slope than the proximity potential would better fit the data. This conclusion is consistent with that of Vaz and Alexander who found it difficult to fit data above and below the Coulomb barrier with the same potential.

Finally we wish to make some considerations of astrophysical interest. At very low energies one can make the approximation $\ln(1 + e^{-2K_0}) \sim e^{-2K_0}$, and then the S factor becomes

TABLE IV. Fusion cross section for $^{16}\text{O} + ^{16}\text{O}$. $\sigma_F^{(1)}$, $\sigma_F^{(2)}$, and σ_F^{prox} are obtained by summing over all significant partial waves. In $\sigma_F^{(1)}$ the barrier is given by Eq. (4) with parameters explained in the text. $\sigma_F^{(2)}$ is like $\sigma_F^{(1)}$ but based on the approximation (5) for the penetrability integral; in σ_F^{prox} the barrier is given by Eqs. (11)–(13); σ_F results from Eq. (10). S is calculated from Eqs. (14) and (10).

E (MeV)	$\sigma_F^{(1)}$ (mb)	$\sigma_F^{(2)}$ (mb)	σ_F (mb)	σ_F^{prox} (mb)	S (b MeV)
9.76	7.371	7.669	7.743	8.482	0.711×10^{24}
8.76	0.645	0.656	0.636	0.610	0.133×10^{25}
7.76	0.285×10^{-1}	0.287×10^{-1}	0.277×10^{-1}	0.239×10^{-1}	0.228×10^{25}
6.76	0.537×10^{-3}	0.539×10^{-3}	0.519×10^{-3}	0.424×10^{-3}	0.368×10^{25}
4.00	0.285×10^{-11}	0.285×10^{-11}	0.273×10^{-11}	0.225×10^{-11}	0.119×10^{26}

TABLE V. Same as Table IV but for $^{14}\text{N} + ^{12}\text{C}$.

E (MeV)	$\sigma_F^{(1)}$ (mb)	$\sigma_F^{(2)}$ (mb)	σ_F (mb)	σ^{prox} (mb)	S (b MeV)
6.07	10.907	11.299	10.889	10.457	0.324×10^{18}
5.07	0.451	0.456	0.435	0.361	0.622×10^{18}
4.07	0.418×10^{-2}	0.418×10^{-2}	0.397×10^{-2}	0.308×10^{-2}	0.108×10^{19}
3.07	0.319×10^{-5}	0.318×10^{-5}	0.300×10^{-5}	0.230×10^{-5}	0.176×10^{19}
1.00	0.396×10^{-24}	0.396×10^{-24}	0.370×10^{-24}	0.305×10^{-24}	0.414×10^{19}

$$S \approx \frac{\hbar^2}{4\mu} \frac{\pi}{D_p + D_c} \exp \left[\frac{\pi(E - E_0)}{\hbar\omega_0} + 4\eta \arcsin \left(\frac{kR_0}{2\eta} \right)^{1/2} + 2[kR_0(2\eta - kR_0)]^{1/2} \right]. \quad (15)$$

Making the derivative with respect to E , one obtains for $E \approx 0$

$$\frac{dS}{dE} \approx \frac{\pi\hbar^2}{4\mu[D_p(0) + D_c(0)]} \left[\frac{\pi}{\hbar\omega_0} - \frac{4}{3} \left(\frac{\mu R_0^3}{2\hbar^2 Z_1 Z_2 e^2} \right)^{1/2} + F \right] \exp \left[-\frac{\pi E_0}{\hbar\omega_0} + \left(\frac{32\mu Z_1 Z_2 e^2 R_0}{\hbar^2} \right)^{1/2} \right], \quad (16)$$

where D_p and D_c have been defined by Eqs. (7) and (8), respectively, and F is a function of the parabola parameters R_0 , E_0 , $\hbar\omega_0$ of the reduced mass μ and the charges Z_1 , Z_2 :

$$F = \frac{3}{2} \frac{1}{\gamma - E_0} - \frac{3\alpha^{1/2}(\gamma - E_0)^{1/2} - \alpha^{3/2}(\gamma - E_0)^{3/2} - (\gamma/E_0 - 1)^{1/2}}{E_0^{1/2}(\gamma - E_0)^{1/2} + [\arcsin(E_0/\gamma)]^{1/2} + \pi/2} \gamma + 2\alpha^{1/2}(\gamma - E_0)^{3/2}. \quad (17)$$

For brevity we have denoted $1/\alpha = Z_1 Z_2 e^2 / R_0$ and $\gamma = \mu \omega_0^2 R_0^2 / 2$. Fixing R_0 and E_0 one can find the value of $\hbar\omega_0$ for which

$$\frac{dS}{dE} = 0, \quad (18)$$

These values are given in the last column of Table I and, if compared with those from column 5 which fit the barrier formed with the proximity potential, they are systematically smaller. As we have mentioned, to have a good fit of the experimental S factor we need even larger values than those in column 5. For such values dS/dE becomes negative close to $E \approx 0$. Within the present model one would therefore expect a monotonically decreasing S at very low energies.

V. CONCLUSIONS

We have derived an analytic formula for the fusion cross section, valid at sub-Coulomb ener-

gies. This is complementary to Wong's formula which can be used around and above the Coulomb barrier. The derivation is based on a model proposed by Avishai to approximate a realistic Coulomb barrier with a half-parabola and a Coulomb potential between two point charges at the left and right of the barrier position, respectively. We have added a centrifugal term and studied various approximations leading to the derived analytic formula. An estimate of the error made by using this compact formula instead of calculating with the exact barrier for each partial wave was made, and it was found that on the average, for energies of 3–4 MeV below the Coulomb barrier, the formula gives a cross section of ~25% higher than the detailed exact calculations. From a comparison with the experimental S factor it was found that the proximity potential modified by Vaz and Alexander to fit fusion data at energies above the Coulomb barrier is inadequate at sub-Coulomb energies where data are quite sensitive to the inner

TABLE VI. Same as Table IV but for $^{10}\text{B} + ^{12}\text{C}$.

E (MeV)	$\sigma_F^{(1)}$ (mb)	$\sigma_F^{(2)}$ (mb)	σ_F (mb)	σ^{prox} (mb)	S (b MeV)
4.22	8.708	8.946	8.466	7.869	0.184×10^{14}
3.22	0.149	0.150	0.140	0.119	0.312×10^{14}
2.22	0.123×10^{-3}	0.123×10^{-3}	0.114×10^{-3}	0.961×10^{-4}	0.482×10^{14}
1.22	0.274×10^{-10}	0.274×10^{-10}	0.251×10^{-10}	0.220×10^{-10}	0.702×10^{14}
0.25	0.153×10^{-42}	0.153×10^{-42}	0.131×10^{-42}	0.131×10^{-42}	0.964×10^{14}

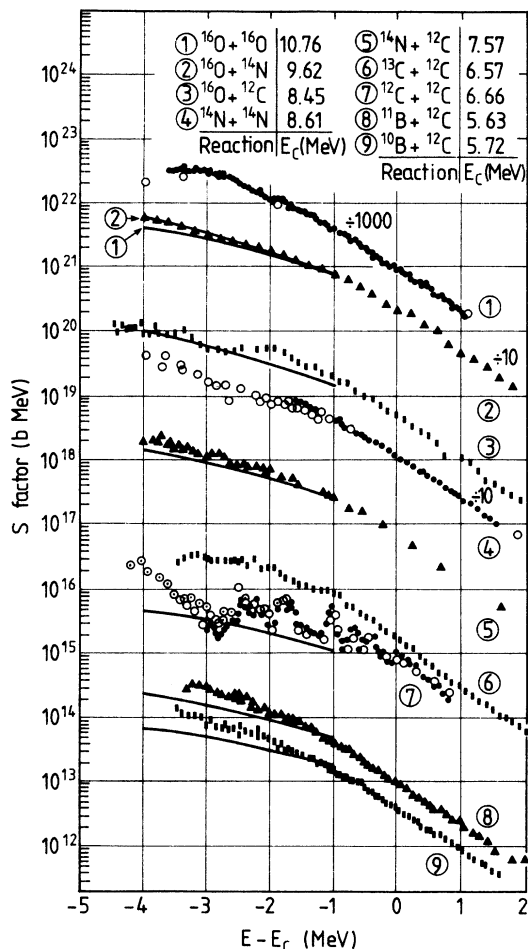


FIG. 3. Comparison between the experimental S factor (Ref. 11) and results of formula (10).

side of the barrier. A nuclear potential with a steeper slope giving rise to a narrower barrier would improve the agreement with the experiment.

ACKNOWLEDGMENTS

One of us (F.S.) is grateful to Dr. D. M. Brink and Dr. A. Babcenco for several fruitful discus-

sions and to Dr. P. E. Hodgson for kind hospitality at the Nuclear Physics Laboratory, Oxford. We would like to thank Prof. L. Wilets for a careful reading of the revised version of this work.

APPENDIX

In this appendix we shall rederive Wong's formula¹⁰ for the fusion cross section, valid at energies around and above the Coulomb barrier. The derivation of our expression (10) follows along the same lines. In both cases the important common feature is that the transmission coefficient is of the form

$$T_l = \frac{1}{1 + b e^{\alpha x^2}}, \quad (\text{A1})$$

where $x = l + \frac{1}{2}$ and b and α depend on the barrier shape. Wong considered barriers of a parabolic shape

$$V_l = E_0 - \mu\omega_0^2 \frac{(r - R_0)^2}{2} + \frac{\hbar^2(l + \frac{1}{2})^2}{2\mu R_0^2} \quad (\text{A2})$$

with the position R_0 and the curvature $\hbar\omega_0$ the same for all partial waves and height $E_l = E_0 + \hbar^2(l + \frac{1}{2})^2/2\mu R_0^2$. From the evaluation of the penetrability integral (3) we obtain in this case

$$b = \exp\left(\frac{2\pi}{\hbar\omega_0}(E_0 - E)\right), \quad \alpha = \frac{\pi\hbar^2}{\hbar\omega_0\mu R_0^2}. \quad (\text{A3})$$

The fusion cross section (1) is calculated under the assumption that one can replace the sum over l with an integral over the variable $x = l + \frac{1}{2}$. Then using expression (A1) for T_l , the cross section becomes

$$\sigma_F = 2\pi\chi^2 \int_0^\infty \frac{x dx}{1 + b e^{\alpha x^2}} = \frac{\pi\chi^2}{\alpha} \ln\left(1 + \frac{1}{b}\right), \quad (\text{A4})$$

which brings us to Wong's formula

$$\sigma_F = \frac{\hbar\omega_0 R_0^2}{2E} \ln\left(1 + \exp\frac{2\pi(E - E_0)}{\hbar\omega_0}\right). \quad (\text{A5})$$

¹L. C. Vaz and J. M. Alexander, Phys. Rev. C **18**, 2152 (1978).

²K. Nagatani and J. C. Peng, Phys. Rev. C **19**, 747 (1979).

³M. Arnould, W. M. Howard, and R. Y. Cusson, Proceedings of the International Workshop on Gross Properties of Nuclei and Nuclear Excitations, Hirschegg, Austria, 1978, edited by H. von Groote (Technische Hochschule Darmstadt report).

⁴K. Siwek-Wilczynska and J. Wilczynski, Phys. Lett. **74B**, 313 (1978).

⁵J. Błocki, J. Randrup, W. J. Swiatecki, and C. F. Tsang, Ann. Phys. (N.Y.) **105**, 427 (1977).

⁶D. L. Hill and J. A. Wheeler, Phys. Rev. **89**, 1102 (1953).

⁷Y. Avishai, Z. Phys. A **286**, 285 (1978).

⁸J. P. Bondorf *et al.*, Phys. Rep. **C15**, 83 (1974).

⁹E. C. Kemble, Phys. Rev. **48**, 549 (1935); see also M. V. Berry and K. E. Mount, Rep. Prog. Phys. **35**, 315 (1972).

¹⁰C. Y. Wong, Phys. Rev. Lett. **31**, 766 (1973).

¹¹R. G. Stokstadt *et al.*, Phys. Rev. Lett. **37**, 888 (1976).